

ROLE OF MICROSTRUCTURE IN MECHANICAL PROPERTIES OF PORCELAIN STONEWARE TILES

V. Biasini, M. Dondi, M. Raimondo, C. Melandri, S. Guicciardi

IRTEC-CNR, via Granarolo 64 – 48018 Faenza, Italy

ABSTRACT

Industrial porcelain stoneware samples were studied and compared with laboratory ones obtained with the addition of glass-ceramics. The addition had been done in bulk, adding glass-ceramic precursors to the standard raw materials. Microstructural and mechanical characterisations were carried out and fracture origin analysis was done in order to identify critical flaws and characterise their size and nature.

The addition of different glass-ceramic systems gives rise to different materials, in a few cases even worsening both texture and mechanical properties, but generally improving the material characteristics and opening the way for further investigations of new mixtures and compositions.

The total porosity of samples not containing glass-ceramics turned out to be in the 2 – 6 vol% range and the glassy phase amount between 46 wt% and 58 wt%. In the glass-ceramic added samples the values were much more scattered, total porosity being between 4 vol% and 14 vol% and amorphous phase amount between 46 wt% and 64 wt%.

The calculated fracture origin size was in the range between 150 μm and 950 μm (see Table 3) for the standard industrial materials. No void or pore or crystal grain of such size were noticed in the microstructure of the fracture surface, so what acted as critical flaw was the link-up of two or more defects close to each other.

In the glass-ceramic added samples the calculated fracture origin size was of the same order of magnitude of the industrial ones, in spite of the higher porosity. So, porosity by itself is not the only responsible for the brittleness but some strengthening effect due to the addition of glass-ceramic has to be claimed.

INTRODUCTION

The ceramic tile production has undergone a sharp growth in recent years, focusing now in particular on products suitable for innovative applications, with great added value, and more and more resistant materials. Porcelain stoneware is a low porosity product with good mechanical properties and therefore it is a running candidate for a broader range of uses, which include external areas^[1,2].

One of the most extensively investigated ways to improve both technical performances and aesthetic characteristics of porcelain stoneware is the addition of glass-ceramics to the body^[3]. Glass-ceramics are polycrystalline materials containing residual amorphous phases, obtained by controlled crystallisation of a molten glassy mass. Some glass-ceramics systems have thermal and chemical stability compatible with the technological requirements of porcelain stoneware production and appropriate mixtures of glass-ceramics and standard raw materials can be treated without relevant changes in productive cycles.

The addition of glass-ceramic precursors to the standard porcelain stoneware leads to final characteristics depending on the nature of the glass-ceramic system used^[4]. To obtain further improvement of mechanical properties of porcelain stoneware it is important to understand mechanisms and features which have detrimental effect on such properties in order to design materials and processes capable to develop the required properties.

The microstructure of this kind of materials tend to be complex, more crystalline phases are present, with an associated glassy phase. A wide range of grain size is observed, generally 1-100 μm . Porosity, which can be fine or coarse, open or closed, is also common^[5]. What's more, each of these microstructural features can act as critical defect, under particular external conditions.

The aim of this study was to investigate the role of microstructure, in particular in terms of defects, in mechanical properties of porcelain stoneware and to assess how and why microstructure, mechanical properties and flaws, change following the addition of glass-ceramics to the bodies.

MECHANICAL BEHAVIOUR OF CERAMICS

The mechanical properties of a material determine its limitations for the applications where the material is required to sustain a load. The theoretical strength of a ceramic material is its strength in absence of flaws and it is generally very high, but these strengths are rarely observed in practice. The common strengths of ceramics are generally several orders of magnitude less than the theoretical values. This is due to the presence of fabrication flaws and structural flaws in the material, which result in fracture at a load well below the theoretical strength. In fact, the presence of flaws such as a crack, pore or inclusion in a ceramic material results in stress concentration when a load is applied. When this concentrated stress at an individual flaw reaches a critical value that is enough to initiate and extend a crack, fracture occurs^[6,7]. Even a small flaw in ceramics is extremely critical, compared to other kinds of materials. For relating the

fracture stress, the material properties and the flaw size, Griffith^[8] proposed an equation of the form:

$$\sigma_f = Y^{-1} (E\gamma_s / c)^{1/2} \quad [1]$$

where σ_f is the fracture stress, E the Young's modulus, γ_s the surface energy, c the flaw size and Y is a constant that depends on the specimen and flaw geometry.

Introducing the fracture energy, γ_{fr} in place of γ_s and, hence, the fracture toughness K_{Ic}

$$\sigma_f = Y^{-1} K_{Ic} / c^{1/2} \quad [2]$$

Thus, the fracture strength depends on the square root of the critical flaw size. If the fracture toughness of the material is known, flaw size can be estimated from the above equation making some assumptions on flaw geometry and position. Equations [1] and [2] established the correlation between strength and microstructure in brittle materials, and they were the theoretical basis from which fractographic analysis was born.

MATERIALS AND METHODS

Four industrial porcelain stoneware tiles and six laboratory samples were studied. The industrial samples had standard porcelain stoneware composition and were called CAE, HEK, OP and NT. The six laboratory samples had been obtained with the addition of 10-30 wt% of glass-ceramic precursors to standard industrial mixtures. The addition had been done in bulk, adding glass-ceramic precursors to the standard raw materials, and the samples were called D31, VC5, R20, 114, DVC19, and PG. The glass-ceramic systems were $\text{Na}_2\text{O}-\text{Al}_2\text{O}_3-\text{SiO}_2$ (NAS), $\text{K}_2\text{O}-\text{CaO}-\text{MgO}-\text{Al}_2\text{O}_3-\text{SiO}_2$ (KCMAS), $\text{BaO}-\text{Al}_2\text{O}_3-\text{SiO}_2$ (BAS), $\text{ZrO}_2-\text{CaO}-\text{SiO}_2$ (ZCS) and $\text{MgO}-\text{Al}_2\text{O}_3-\text{SiO}_2$ (MAS).

Phase composition was determined by RIR-XPRD (Rigaku Miniflex, Ni-filtered $\text{Cu K}\alpha$). Open porosity, water absorption and bulk density were measured according to ISO EN 10545-3. Total porosity was determined on the basis of the ratio between bulk density and specific weight of the ceramic material (ASTM C329); closed porosity was calculated by difference.

The Young's modulus and the Poisson's ratio were measured by resonant frequency method on specimens $70 \times 2 \times 10 \text{ mm}^3$, length \times thickness \times width, respectively, according to ENV 843-2. The four-point flexural strength was measured on specimens $45 \times 3 \times 4 \text{ mm}^3$, length \times thickness \times width, respectively, according to ENV 843-1, using an Instron machine mod. 1195. The fracture toughness was measured, on the same machine, by the Single Edge Notched Beam (SENB) method on specimens $25 \times 4 \times 3 \text{ mm}^3$, length \times thickness \times width, respectively, and a saw cut 0.1 mm wide and 1.2 mm deep, using a four-point bending device with a lower span of 20 mm and an upper span of 10 mm. The Vickers hardness was measured on polished surfaces according to the European Standard EN 843-4, using a hardness testing machine Zwick 3212 with an applied load of 9.8 N.

The calculated fracture origin size was determined from equation [2] with the shape factor $Y=1.3$ ^[9] for semicircular surface flaws. The fractographic analysis was done on specimens fractured in flexural strength tests. The specimens were mounted with the tensioned surfaces in contact and the fracture surfaces were analysed by Scanning Electron Microscope (Cambridge Stereoscan 360).

RESULTS AND DISCUSSION

INDUSTRIAL MATERIALS

Phase composition, porosity values and mechanical properties of industrial materials are reported in Tables 1-3. The main crystalline phases were quartz and mullite, then plagioclase, zircon, corundum and cristobalite. HEK and OP showed some residual K-feldspar. Most of these values ranged around 55-58 wt% while NT showed a sensibly lower value (46 wt%), however in the common range for porcelain stoneware^[1, 10]. At the same time, NT contains more closed porosity, let's say residual porosity, that was not filled, during the firing treatment, at the same extent as in samples containing more amorphous phase. The open porosity was almost the same in all the samples. All the tested tiles had been lapped and the open pores came from the removal of the as-fired surface during the lapping process.

Phase [wt%]	CAE	HEK	OP	NT
Mullite	8.2 ± 1.5*	11.4 ± 1.5	13.6 ± 1.7	8.8 ± 1.8
Quartz	28.2 ± 1.7	24.1 ± 1.8	22.4 ± 1.7	28.3 ± 1.0
Cristobalite	0.8 ± 0.0	0.6 ± 0.1		1.8 ± 0.1
Plagioclase	2.7 ± 0.0	0.9 ± 0.1	0.4 ± 0.0	3.8 ± 0.1
K-feldspar		0.7 ± 0.1	0.3 ± 0.0	
Zircon	4.2 ± 1.1	1.3 ± 0.4	2.4 ± 0.4	7.9 ± 0.4
α-Al ₂ O ₃	0.9 ± 0.1	2.8 ± 0.7	3.4 ± 0.5	3.4 ± 0.3
Amorphous phase	55.0 ± 2.2	58.0 ± 2.4	57.0 ± 2.0	46.0 ± 3.2

* Mean ± 1 standard deviation.

Table 1. Phase composition of the industrial materials.

	CAE	HEK	OP	NT
Open porosity [vol%]	0.3 ± 0.1*	0.2 ± 0.1	0.2 ± 0.1	0.2 ± 0.1
Closed porosity [vol%]	3.7 ± 0.2	4.1 ± 0.1	1.6 ± 0.1	5.8 ± 0.2
Total porosity [vol%]	4.0 ± 0.2	4.3 ± 0.1	1.8 ± 0.1	6.0 ± 0.2

* Mean ± 1 standard deviation.

Table 2. Porosity values of the industrial materials.

	CAE	HEK	OP	NT
Flexural Strength [MPa]	33.3 ± 1.6*	29.0 ± 1.4	40.2 ± 1.2	76.7 ± 3.3
Calculated mean fracture origin size (µm)	690	950	530	150
Young's Modulus [GPa]	64 ± 1	63 ± 1	71 ± 1	72 ± 1
Poisson's ratio	0.18	0.18	0.18	0.18
Fracture Toughness [MPa m ^{0.5}]	1.14 ± 0.04	1.16 ± 0.06	1.20 ± 0.05	1.21 ± 0.05
Vickers Hardness [GPa]	6.4 ± 0.4	5.6 ± 0.6	6.8 ± 0.5	5.9 ± 0.4

* Mean ± 1 standard deviation.

Table 3. Mechanical characterisation results of the industrial materials.

The influence of amorphous phase content on flexural strength is illustrated in Figure 1. The amorphous phase has a weakening effect. Sample NT, with the lowest amorphous content showed the highest flexural strength value (76.6 MPa), almost the double of the OP value (40.2 MPa). Both Young's modulus and fracture toughness values were slightly higher in NT, the sample with the lowest amorphous phase content, but this is not sufficient to explain the much higher flexural strength. Moreover, the expected detrimental effect of porosity on flexural strength and Young's modulus was not detected in sample NT. On the contrary, it seems that both flexural strength and Young's modulus are more affected by amorphous phase amount than by residual porosity.

Finally, the Poisson's ratio was the same for all the materials, being evidence for the similar nature of the samples. The excellent characteristics of NT were only spoiled by the Vickers hardness, 5.9 GPa, even if still in good agreement with literature data^[11-13].

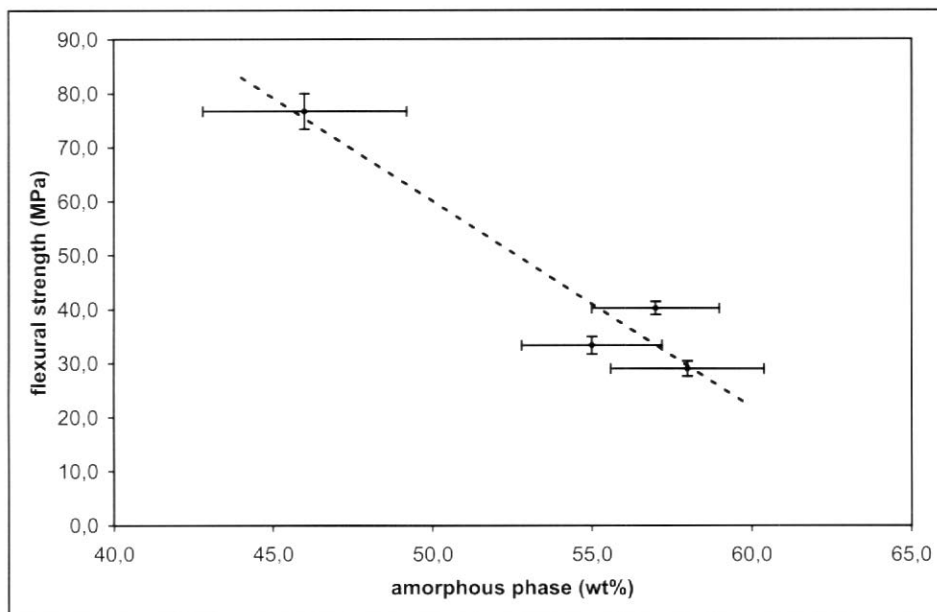


Figure 1. Influence of amorphous phase content on flexural strength of industrial tiles.

The reason of the different strength values was investigated by means of fractographic analysis. Fracture analysis or fractography is the examination of the fractured specimen in an effort to reconstruct the sequence and cause of fracture. It helps to determine why and where the failure occurred and the nature, size and location of the flaw which acted as fracture origin. Unfortunately, low fracture energies as those found in coarse-grained or porous ceramics, like the samples we were dealing with, hardly leave distinct fracture markings. Anyway, with the help of the calculated fracture origin size, in some cases we were able to detect the general region of the fracture origin, and to identify, locate and measure the flaw from which the fracture started. At the same time, the microstructural characterisation of the fracture surfaces was performed.

In Fig. 2 a comparison among the fracture surfaces of the industrial samples is shown. The microstructure of HEK and OP, containing the highest amount of amorphous phase, had a glassy appearance characterised by the presence of many bubbles, up to 50 μm in size, while NT had the most crystalline microstructure.

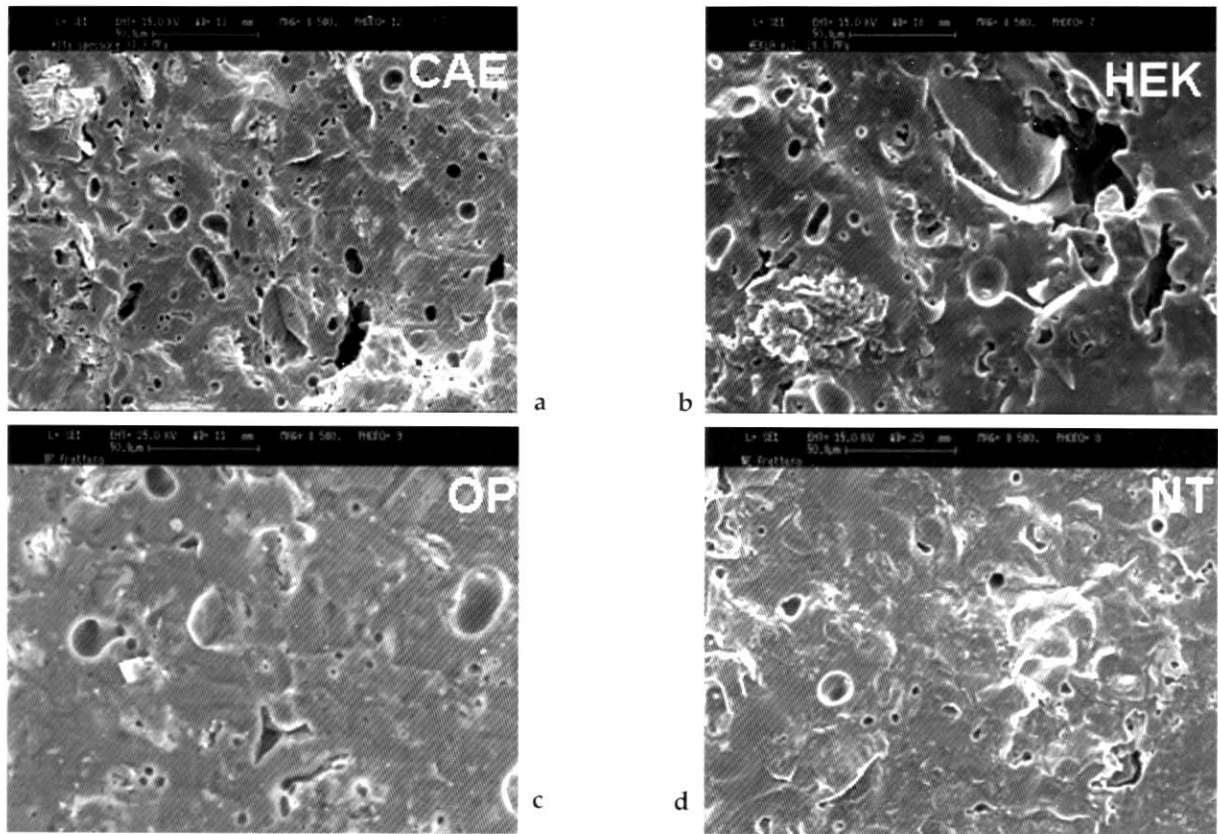


Figure 2. Microstructure of the fracture surfaces of the industrial samples.

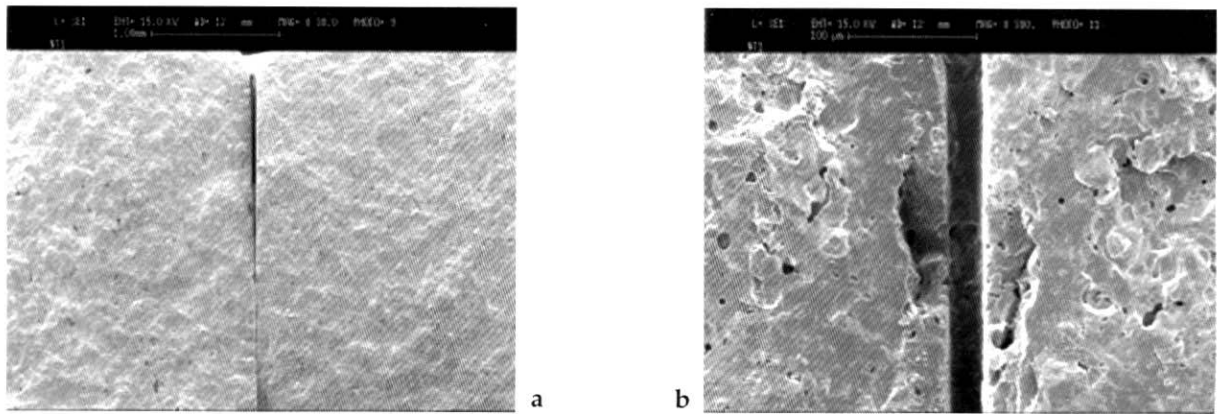


Figure 3 a, b. SEM images of NT flexure bar fractured at 77.7 MPa.

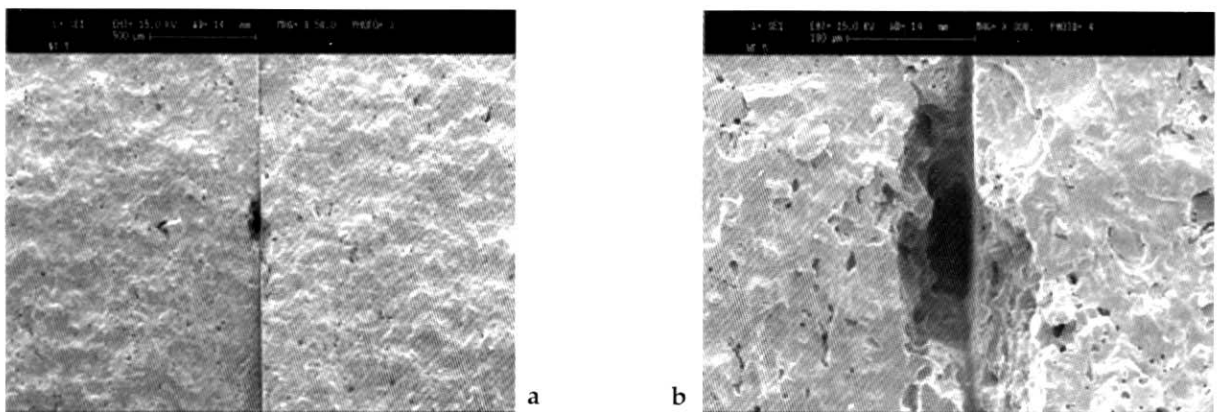


Figure 4 a, b. SEM images of NT flexure bar fractured at 75.4 MPa.

NT flexure specimens mainly broke because of surface located flaws, 100-150 μm in size, as shown in Figs. 3 and 4. The size of the detected fracture origins agreed well with the calculated fracture origin size. Cavities of that size were frequently present in the bulk material, but the surface ones were the more critical with regard to the failure in bending tests.

The agreement between calculated and detected fracture origin size was less clear in the other samples. The calculated size was between 530 and 950 μm , and the fractured surface appearance was mostly as the ones shown in Figs. 5 and 6.

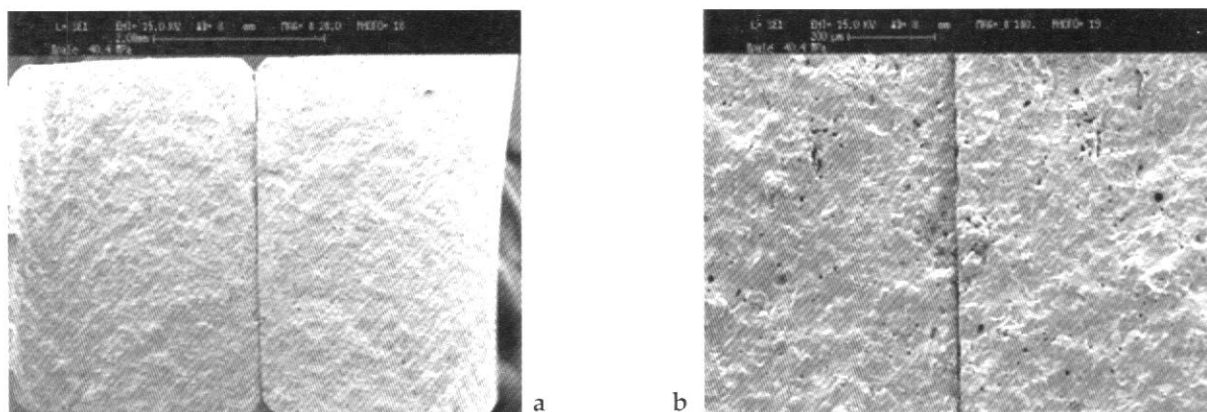


Figure 5. SEM images of the OP flexure bar fractured at 40.4 MPa.

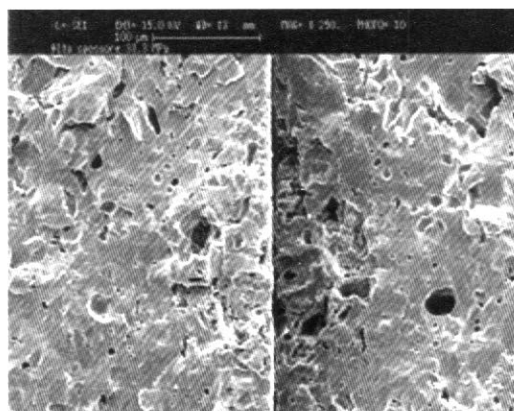


Figure 6. Fracture origin in CAE flexure bar fractured at 33.3 MPa.

The detected flaws were pore aggregates at maximum 200 μm in size. However, the severity of the strength reduction, together with the estimated fracture origin size, and the rough and porous microstructure of the samples, allows to suppose that defects close together, such as pores or big crystalline grains, interacted and behaved like a much larger flaw that resulted in much lower strength. In that case the intact material between the flaws cracked first, the defects linked and the real defect size was the sum of the individual sizes and the distance between them.

• LABORATORY SAMPLES

Phase composition, porosity values and mechanical properties of the laboratory samples containing glass-ceramics, are shown in Tables 4-6. Phase composition depended on the type of glass-ceramic system added to the industrial mixtures. NAS and KCMAS addition did not influence the nature of crystalline phases, producing increases of

amorphous phase, up to 60 wt% in D31 and 64 wt% in R20, that did not result in any lowering of the porosity content. Bodies containing ZCS, BAS and ZCS-BAS systems developed some phases, unusual in standard porcelain stoneware, such as $\text{Ca}_2\text{ZrSi}_4\text{O}_{12}$ in VC5 and DVC19 and $\text{BaAl}_2\text{Si}_2\text{O}_8$ (celsian) in 114 and DVC19 samples. The latter material, in particular, turned out to consist mainly (31.0 wt%) of celsian. In all of them lower amounts of glassy phase and higher porosity content were detected, compared with both industrial and D31 and R20 bodies. The glass-ceramic addition in samples 114 and VC5, BAS and ZCS systems respectively, had detrimental effect on mechanical properties and densification behaviour. The addition of a mixture of ZCS and BAS systems, as in DVC19, caused better densification and mechanical properties in comparison with the previous samples, added with the two glass-ceramic systems, but separately. DVC19 showed the highest Young's modulus value (74 GPa) as well as flexural strength and fracture toughness comparable with the industrial products, notwithstanding the significant residual porosity (7.4 vol%). The Poisson's ratio of this sample (0.26) considerably differed from the others, probably because of the very different phases developed in the material.

Phase [wt%]	D31 (NAS)	R20 (KCMAS)	VC5 (ZCS)	DVC19 (ZCS-BAS)	114 (BAS)	PG (ZCS-MAS)
Mullite	7.1 ± 1.5*	6.5 ± 1.0	7.5 ± 1.8	8.2 ± 1.6	8.3 ± 1.9	6.3 ± 1.9
Quartz	25.5 ± 1.4	24.1 ± 1.7	17.4 ± 0.9	3.5 ± 0.2	24.3 ± 0.3	24.7 ± 1.6
Cristobalite	0.2 ± 0.0	0.3 ± 0.0		1.0 ± 0.1	1.2 ± 0.1	0.9 ± 0.1
Plagioclase	3.3 ± 0.0	3.3 ± 0.1	3.4 ± 0.1	1.6 ± 0.2	2.8 ± 0.2	3.0 ± 0.1
K-feldspar	0.8 ± 0.1	0.9 ± 0.1	0.8 ± 0.1			
Celsian				31.0 ± 3.2	15.5 ± 4.1	
Zircon	0.4 ± 0.2	0.5 ± 0.1	10.3 ± 0.5			10.7 ± 0.8
$\text{Ca}_2\text{ZrSi}_4\text{O}_{12}$			8.2 ± 0.9	3.0 ± 0.4		
$\alpha\text{-Al}_2\text{O}_3$	2.5 ± 0.3			2.8 ± 0.4	2.0 ± 0.0	
Amorphous phase	60.0 ± 1.4	64.0 ± 1.4	52.4 ± 2.0	48.8 ± 1.0	46.0 ± 0.6	54.4 ± 2.5

* Mean ± 1 standard deviation

Table 4 Phase composition of the laboratory samples containing glass-ceramics.

	D31	R20	VC5	DVC19	114	PG
Open porosity [vol%]	0.0	0.4 ± 0.8*	1.5 ± 0.7	0.1 ± 0.2	5.8 ± 1.0	0.04 ± 0.03
Closed porosity [vol%]	3.7 ± 0.5	4.0 ± 1.5	13.0 ± 1.4	7.3 ± 0.3	6.0 ± 1.9	7.6 ± 0.5
Total porosity [vol%]	3.7 ± 0.5	4.4 ± 1.5	14.5 ± 1.4	7.4 ± 0.3	11.8 ± 1.9	7.7 ± 0.5

* Mean ± 1 standard deviation.

Table 5 Porosity values of the laboratory samples.

	D31	R20	VC5	DVC19	114	PG
Flexural Strength [MPa]	39.1 ± 1.3*	42.8 ± 1.7	25.8 ± 0.7	39.7 ± 2.2	28.7 ± 1.0	76.6 ± 3.0
Calculated mean fracture origin size[μm]	580	440	770	400	760	150
Young's Modulus [GPa]	69 ± 1	73 ± 1	51 ± 1	74 ± 1	51 ± 1	70 ± 1
Poisson's ratio	0.19	0.18	0.21	0.26	0.18	0.19
Fracture Toughness [$\text{MPa m}^{0.5}$]	1.22 ± 0.04	1.17 ± 0.03	0.93 ± 0.03	1.03 ± 0.05	1.03 ± 0.07	1.20 ± 0.04
Vickers Hardness [GPa]	5.8 ± 0.5	6.8 ± 0.5	5.0 ± 1.1	5.4 ± 0.5	5.0 ± 0.5	6.0 ± 0.5

* Mean ± 1 standard deviation.

Table 6 Mechanical characterisation results of the laboratory samples.

R20 (KCMAS) had quite high Young's modulus (73 GPa), higher than in standard bodies, and flexural strength (42.8 MPa) similar to the average in standard materials. The addition of NAS system in D31 did not cause any improvement regarding either mechanical properties or residual porosity. PG had the highest flexural strength, almost the double of the strength of R20 together with almost the double of residual porosity, and good Young's modulus, fracture toughness and hardness. Moreover, it showed the same strength of NT standard body, though it contained higher porosity and more amorphous phase.

The very porous microstructure (Fig. 7a and b) of 114 and VC5 was responsible for the very bad mechanical properties. Furthermore, it made unfruitful any effort to locate the fracture origin in those samples. The calculated fracture origin size was about 770-760 μm for both 114 and VC5, that means flaw size of approximately 1/4 the specimen thickness.

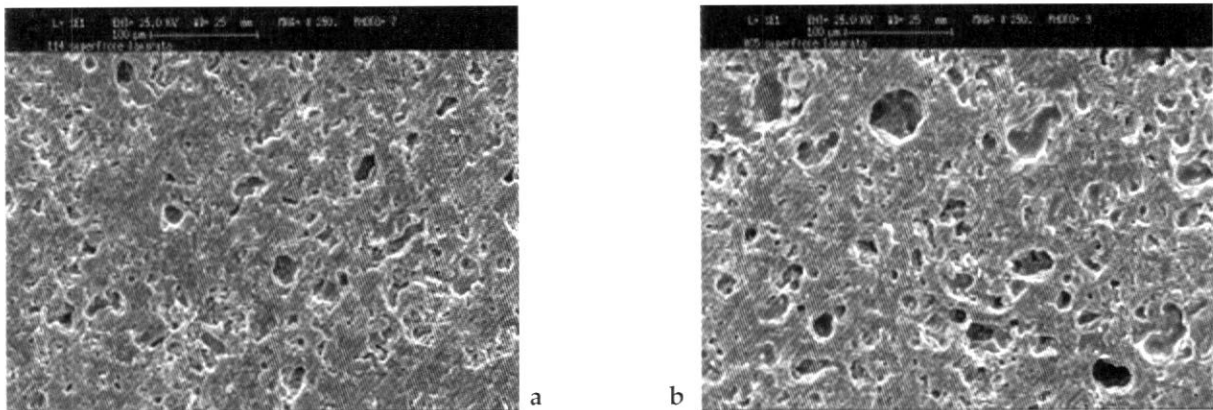


Figure 7. Microstructure of the most porous samples: 114 and VC5.

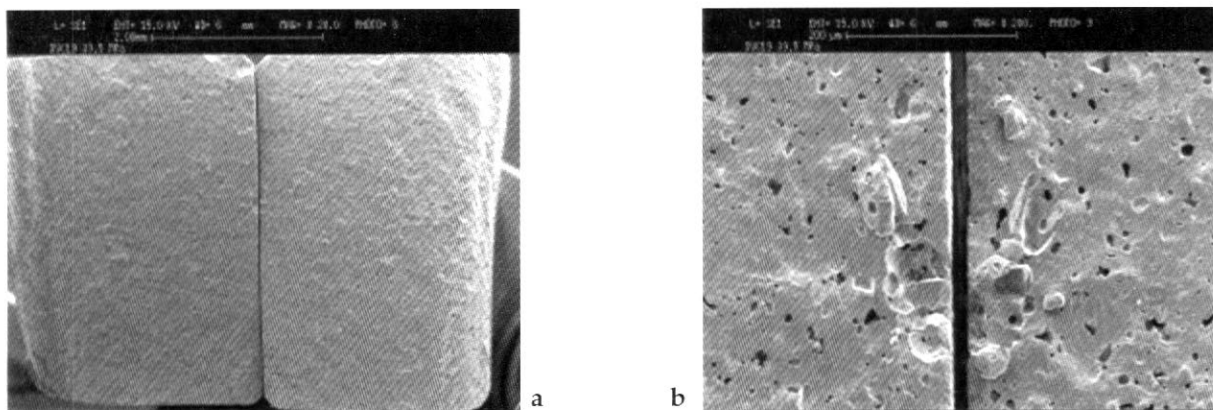


Figure 8. SEM images of the DVC19 flexure bar fractured at 39.5 MPa.

DVC19 microstructure was less porous than the previous ones (Fig. 8a, b), showing maximum pore size of about 30 μm . The calculated flaw size resulted 400 μm for this material, but the detected fracture origins consisted of superficial big grains of about 100-150 μm , close together to make up flaws 300 μm big. Again, some merging between close defects must be responsible for the specimen failure at such low stress.

The PG sample (Figs. 9-10), with excellent mechanical properties, flexural strength at the top, showed a microstructure characterised by scattered elongated internal voids 150-200 μm in size, defects probably arising from incorrect forming process. Among them, the defects closer to the flexure surface acted as fracture origin and started the failure process. The size of such fracture origins matched with the calculated size.

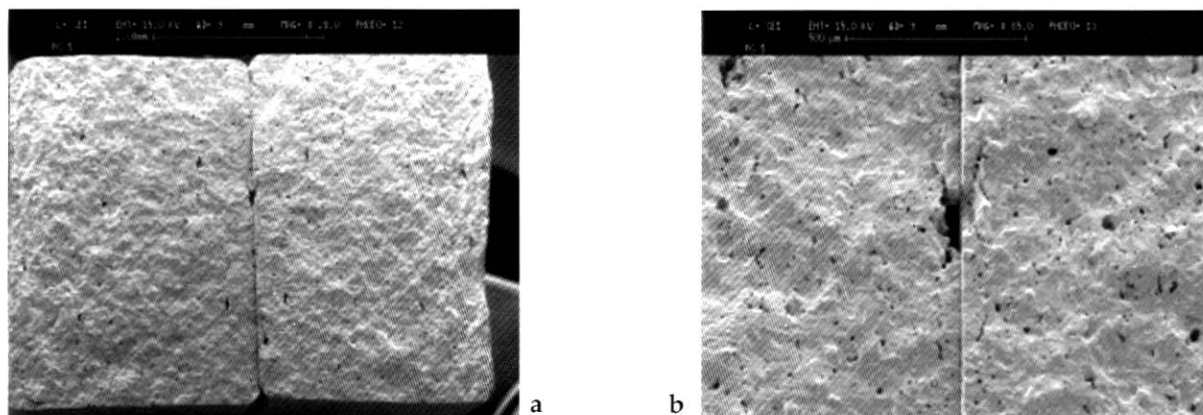


Figure 9 a, b. SEM images of PG flexure bar fractured at 79.0 MPa.

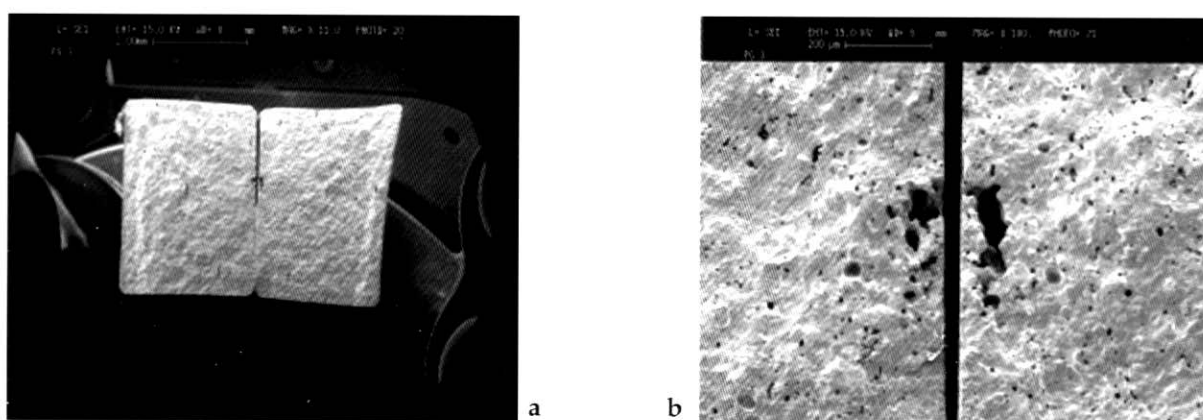


Figure 10 a, b. SEM images of PG flexure bar fractured at 75.2 MPa.

CONCLUSIONS

For similar porcelain stoneware compositions, such as samples CAE, HEK, OP and NT, the influence of amorphous phase amount on flexural strength follows an inversely proportional relation. Between amorphous phase and porosity a so clear correlation was not found, and neither between amorphous phase and Young's modulus. In fact, among the industrial samples, the one with the highest porosity content showed, at the same time, the highest flexural strength and Young's modulus.

The addition of different glass-ceramic systems gives rise to different materials, in a few cases even worsening both texture and mechanical properties, but generally improving the material characteristics and opening the way for further investigations of new mixtures and compositions.

The low fracture energy, characteristic of this kind of materials, makes it difficult to perform fractographic analysis. Anyway, in some cases, in specimens with higher flexural strength, it is possible to identify and measure the fracture origin flaw and compare the result with the calculated fracture origin size. In most samples the data do not match and the detected flaw size is usually half the calculated one. It means that bridges between defects close together cracked and the resulting much larger flaw is responsible for the flexural strength value. The size of the detected fracture origin well agreed with the calculated one only in two samples, the ones with the highest strength. Notwithstanding the number of initial defects present in these materials and their size, often bigger than the initial defects in other samples, the resulting strength was the highest because they do not tend to link up and form larger critical flaws.

REFERENCES

- [1] M. DONDI, G. ERCOLANI, C. MELANDRI, C. MIGAZZINI, M. MARSIGLI *The chemical composition of porcelain stoneware tiles and its influence on microstructural and mechanical properties*, *Interceram* 48 (1999) 75-83.
- [2] L. ESPOSITO, A. TUCCI, A. ALBERTAZZI, E. RASTELLI, *Caratterizzazione fisico-meccanica di un impasto da gres porcellanato*, *Cer. Acta* 8 (1996) 11-19.
- [3] G. BALDI, D. BISERNI, E. GENERALI, D. MAZZINI and D. SETTEMBRE BLUNDO, *Il grès vetroceramico: aspetti scientifici e tecnologici di una nuova classe di materiali*, *Ceramica Informazione* 396 (2000) 262-268.
- [4] V. BIASINI, M. DONDI, S. GUICCIARDI, C. MELANDRI, M. RAIMONDO, E. GENERALI, D. SETTEMBRE BLUNDO, *Mechanical Properties of Porcelain Stoneware Tiles: the Effect of Glass-Ceramic System*, *Key Engineering Materials* 206-213 (2002) 1799-1802.
- [5] C. LEONELLI, F. BONDIOLI, P. VERONESI, M. ROMAGNOLI, T. MANFREDINI, G. C. PELLACANI, V. CANNILLO, *Enhancing the Mechanical Properties of Porcelain Stoneware Tiles: a Microstructural Approach*, *J. Eur. Ceram. Soc.* 21 (2001) 785-793.
- [6] R.W. DAVIDGE, *Mechanical Behaviour of Ceramics*, Cambridge University Press, 1979.
- [7] D. W. RICHERSON, *Modern Ceramic Engineering*, Marcel Dekker, Inc., 1982.
- [8] A.A. GRIFFITH, *The phenomenon of Rupture and Flow in Solids*, *Philos. Trans., Royal Soc. London Ser.*, A221(4) (1920) 163.
- [9] J.J. SWAB, G. QUINN, *Fractography of Advanced Structural Ceramics: Results from the VAMAS Round Robin Exercise*, Army Research Laboratory Report, December 1994.
- [10] L. J. M. G. DORTMANS AND A. P. S. REYMER, *Strength of Ceramic Tiles*, Proceedings of QUALICER 1998, P. GI-225-231.
- [12] A.TUCCI, L. ESPOSITO, *Pulimentacion de baldosas de gres porcelanico: aspectos superficiales*, *Tecnica Ceramica* (2000) 1268-1275.
- [13] L. ESPOSITO, A. TUCCI, D. NALDI, L. RIGHINI, *Le superfici del gres porcellanato*, *Cer. Acta* 12 (2000) 40-52.
- [14] L. ESPOSITO, A. TUCCI, *Porcelain stoneware tile surfaces*, *Am.Ceram.Soc.Bull.*79 (2000) 59-63.